

Colossal Magnetoresistance is a Griffiths Singularity

M. B. Salamon, P. Lin

Department of Physics

University of Illinois

1110 West Green Street, Urbana, IL 61801-3080

S. H. Chun

Department of Physics

Pennsylvania State University

University Park, PA 16802-6300

(November 14, 2018)

It is now widely accepted that the magnetic transition in doped manganites that show large magnetoresistance is a type of percolation effect. This paper demonstrates that the transition should be viewed in the context of the Griffiths phase that arises when disorder suppresses a magnetic transition. This approach explains unusual aspects of susceptibility and heat capacity data from a single crystal of $\text{La}_{0.7}\text{Ca}_{0.3}\text{MnO}_3$.

The term “colossal magnetoresistance” (CMR) has commonly been used to describe the very large, magnetic-field driven changes in electrical resistivity in oxides based on LaMnO_3 near their second-order, ferromagnetic transitions. The largest CMR effects are accompanied by other anomalies in magnetic and thermodynamic properties. Among these are the failure of the magnetic correlation length to increase strongly as the transition temperature T_C is approached from above, the persistence of a well defined spin-wave dispersion close to the transition [1], and an unusual shift in the heat capacity peak to higher temperatures in applied magnetic fields. [2] An explanation of this unusual behavior of the heat capacity in the context of a Griffiths singularity [3] is the focus of the present paper.

There is now general consensus that the CMR transition is a type of percolation in which, due to the double-exchange process [4], bonds become metallic as neighboring spins tend to align. The strength of the CMR effect (along with the transition temperature) depends strongly on the ionic size and concentration of the divalent atom that substitutes for La in LaMnO_3 . The effect is nearly absent for $\text{La}_{2/3}\text{Sr}_{1/3}\text{MnO}_3$ ($T_C = 360$ K) but quite strong in the present sample $\text{La}_{0.7}\text{Ca}_{0.3}\text{MnO}_3$ ($T_C = 218$ K) [5]. In the low temperature metallic phase, the exchange interactions, as measured by the spin-wave stiffness, are the same in Sr- and Ca-doped crystals [6], demonstrating that the key to the CMR effect is to be found in the non-metallic regime. The ionic size of the divalent substituent exerts its effect on magnetic and electronic properties through local tilting of the oxygen octahedra [7] and the concurrent bending of the active Mn-O-Mn bonds. This inhibits the formation of metallic bonds and leads to charge localization, polaron formation, and possible charge segregation [8,9]. Evidence in favor of a percolation picture comes from a Monte-Carlo simulation

of a random field Ising model that assigns conductivity zero and unity to bonds between neighboring antiparallel and parallel spins respectively [10]. It both produces CMR and emphasizes the importance of randomness. Experimental evidence was provided by Jaime et al. [11] who extracted the field and temperature dependent metallic-bond concentration $c(H, T)$ from the resistivity via the effective medium approximation, and showed that it also describes the thermoelectric power data. Direct evidence for coexisting polaronic/insulating and metallic components have been reported from neutron [12], [13], electron [14] and Raman scattering [15] studies.

Discussions of the CMR effect in percolation terms [16–18] have generally neglected a central point: that the percolating entities are formed *thermodynamically* as the temperature is lowered, nucleated by the intrinsic randomness of a doped material and amplified by the tendency for polaron formation and charge segregation [19]. Griffiths [3] first pointed out, in the context of dilution (bonds randomly assigned values of 0 or J), that singularities arise in thermodynamic properties in the temperature range $T_C^{\text{rand}} \leq T \leq T_G$ between the random transition T_C^{rand} and the “pure” transition temperature T_G . Bray [20,21] extended the argument to any bond distribution that reduces the transition temperature, terming the regime between T_C^{rand} and T_G the “Griffiths phase.” In this paper, we use the Bray model to demonstrate that the zero-field transition is an example of a Griffiths singularity. To treat the field dependence, we consider two possible exchange energies: J_{met} , associated with the double-exchange process on metallic Mn-O-Mn bonds, and J_{ins} , the residual ferromagnetic interaction that exists on insulating bonds. The proportion of metallic bonds changes with field and temperature, monitored through the resistivity-based metallic fraction $c(H, T)$.

Among the effects that characterize the Griffiths phase

are a distribution of susceptibilities and slow spin dynamics. The latter have been observed by muon relaxation [22,23] and show up strongly in noise measurements [24]. We focus in this work on the nature of the susceptibility and magnetization, and on the behavior of the heat capacity in applied magnetic fields, tying the last to the CMR effect itself. Figure 1 shows the inverse susceptibility $\chi^{-1}(T) = H/M(T)$ of a single crystal sample of $\text{La}_{0.7}\text{Ca}_{0.3}\text{MnO}_3$, where $M(T)$ is the magnetization in a field of 1 kOe. The high-temperature behavior is of Curie-Weiss form, with a paramagnetic Curie temperature $\Theta = 202$ K. Well above $T_C = 218$ K the slope of the experimental curve corresponds to $S \approx 8$, much shallower than the Curie-Weiss law for spin $S_{eff} = 1.85$ (the weighted average of $S = 3/2$ and $S = 2$ appropriate for this sample), shown as a dashed line. Further, there is a sharp downturn in $\chi^{-1}(T)$ before the Curie temperature is reached. This alone identifies the transition as a Griffiths singularity, characterized by a susceptibility exponent less than unity [25]; that is, $\chi^{-1}(T) \propto (T - T_C^{rand})^{1-\lambda}$, with a non-universal positive exponent $\lambda \leq 1$.

In his treatment of the Griffiths phase, Bray [20,21] argues that the distribution of cluster sizes can be characterized by the longitudinal susceptibility matrix $\chi_{ij} = g^2 \mu_B^2 \langle S_i^z S_j^z \rangle / k_B T$ or rather by its inverse, whose eigenvalues μ/C are distributed according to $p(\mu)$, where

$$p(\mu) \propto \mu^{-\gamma} e^{-A(T)/\mu}. \quad (1)$$

Here C is the Curie constant of the material and each μ represents an effective Curie-Weiss temperature difference $T - \Theta_{eff}(T)$. The $\Theta_{eff}(T)$ may be equally well related [20] to the eigenvalue distribution of the exchange matrix which the double-exchange mechanism makes temperature and field dependent. The close connection between the effective exchange energy and the metallicity of the corresponding Mn-O-Mn bond ties the Griffiths behavior to the CMR effect. Bray ignored the negative-power prefactor, but it is required if $p(\mu)$ is to decrease for large μ and to rise sharply near $\mu = 0$ as T_C^{rand} is approached [20]. As all clusters are finite, none is fully ferromagnetic so we must have $p(\mu \rightarrow 0) = 0$. However, there is a pile-up of large clusters as the transition is approached, leading Bray to deduce that $A(T)$ vanishes as,

$$A(T) = T_0 \left(\frac{T - T_C^{rand}}{T_C^{rand}} \right)^{2(1-\beta)}, \quad (2)$$

where T_0 is a parameter and $\beta = 0.38$ is the order-parameter exponent for the pure system, assumed to be 3D Heisenberg-like. Because $\mu = T$ for free spins, we cut off the distribution $p(\mu)$ and calculate the average inverse susceptibility $\langle \mu \rangle / C$, using

$$\langle \mu \rangle = \frac{\int_0^T \mu p(\mu) d\mu}{\int_0^T p(\mu) d\mu} \quad (3)$$

The result is shown as a solid line in Fig. 1, where the Curie constant is

$$C = \frac{Ng^2 \mu_B^2 S_{eff}(S_{eff} + 1)}{3k_B} = 0.074 \text{ K} \quad (4)$$

and $T_C^{rand} = 223$ K. The free parameters are the characteristic temperature $T_0 = 9.5$ K and the non-universal prefactor exponent, $\gamma = 1.59 \pm 0.5$. The calculated curve is very close to the power law $\chi^{-1}(T) \propto (T - T_C^{rand})^{0.72}$, so that $\lambda = 0.28$, as seen in the inset to Fig. 1. The values of T_0 and γ are strongly correlated; the data can be fit with values of γ in the range cited, resulting in values of λ in the range $0.2 \leq \lambda \leq 0.3$. Analysis of the quantum critical point of UCu_4Pd in terms of a Griffiths singularity yields the much larger value $\lambda = 2/3$ [25].

The downturn in the $\chi^{-1}(T)$ data close to the transition temperature is more abrupt than Bray's approach predicts and T_C^{rand} is somewhat higher than $T_C = 218.2$ K, the location of the zero-field heat capacity peak shown in Fig. 2 [2] that we take to mark the true transition temperature. Griffiths, in his original paper [3], suggested that the susceptibility would tend to diverge in advance of the onset of true long range order, and that may explain the present result. The nonanalytic behavior of the magnetization at small magnetic fields is readily observable in the vicinity of T_C where the magnetization rises so abruptly that, considered in terms of conventional critical behavior $M \propto H^{1/\delta}$, it requires $\delta \approx 13$, far from any standard value. Magnetization data taken at 218 K, showing this rapid rise, are shown in Fig. 3. The upward curvature in the $\chi^{-1}(T)$ data at high temperatures has also been reported by, for example, de Teresa et al. [26], who find a linear regime at high temperatures with a slope consistent with the Curie constant in Eq.(4) and an effective Curie-Weiss temperature $\approx 1.25T_C$; it is tempting to assign this to T_G .

Figure 2 shows the heat capacity of the sample in fields of 0 T, 3 T and 7 T after subtraction of a smooth background that fits the data at temperatures well away from the peak. The sharpness of the zero field data might signal a first-order transition, but there is no evidence of hysteresis. The shift in the heat capacity peak is uncharacteristic of ferromagnetic transitions, as discussed previously [2]. To treat this behavior, we employ a modified version of the Oguchi cluster method [27], a simple improvement to mean-field theory. In this method, the energy of a pair is treated exactly, while coupling to its $z - 1$ neighbors is handled in mean-field theory. The magnetic part of the double-exchange energy is $xt[\cos(\theta/2) - \overline{\cos(\theta/2)}]$, where θ is the classical angle between core spins, t is the transfer energy, x is the doping level and the bar denotes the angular average. For the Oguchi calculation, we use the quantum analog [28]

$$E_{de}(S_0) = xt \left[\frac{S_0 + 1/2}{2S + 1} - \overline{\frac{S_0 + 1/2}{2S + 1}} \right], \quad (5)$$

where S_0 , the total spin of the two manganese $S_c = 3/2$ cores and the shared e_g electron, is in the range $1/2 \leq S_0 \leq 7/2$. The pair is coupled to the magnetization of its $z-1$ neighbors via either metallic J_{met} or insulating J_{ins} exchange bonds. Assuming spherical clusters (of undetermined size), we follow the effective-medium approach of Jaime, et al. [11] and extract the metallic bond concentration $c(H, T)$ from the measured resistivity $\rho(H, T)$ (Fig. 2a) by extrapolating the fitted the high-temperature (activated) and low temperature (power-law) resistivities. The resulting $c(H, T)$ is shown for several applied fields in Fig. 2b. The effective field acting on the pair is, then,

$$H_{eff} = H + 2(z-1)S_{eff}J_{eff}m(H, T)/g\mu_B, \quad (6)$$

where $m(H, T)$ is the reduced magnetization, to be calculated self-consistently, and $J_{eff} = c(H, T)J_{met} + [1 - c(H, T)]J_{ins}$. The resultant $m(H, T)$ values are then used to determine the pair energy $\langle E_{de}(S_0) \rangle$ within the Oguchi approach.

The field and temperature dependent heat capacity calculated from $\langle E_{de}(S_0) \rangle$ with a single amplitude parameter, shown as solid lines in Fig. 2c, is in good agreement with the data. The insulating exchange energy is determined from the observed Curie constant to be $J_{ins} = 3k_B\Theta/2zS_{eff}(S_{eff} + 1) = 0.82$ meV. We obtain the transfer energy t from the spin-wave stiffness D according to $t \approx (2S_c + 1)D/xa^2$ [29]. The energy difference between parallel and antiparallel configurations is $E_{de}(7/2) - E_{de}(1/2) = 3xt/5$; for a Heisenberg interaction $-2J_{met}\vec{S}_1 \cdot \vec{S}_2$ the difference would be $4S^2J_{met}$ giving $J_{met} = 3xt/20S^2$. For $D = 150$ meV \AA^2 , which is common to most manganites at this doping level [6], we find $t = 130$ meV and $J_{met} = 1.46$ meV. Clearly, the background subtracted from the data has ignored magnetic contributions that remain well below T_C . The shoulder in the zero-field curve arises from the tail in $c(0, T)$ in the vicinity of T_C . This may signal a break-down in the effective medium approximation, as very large clusters are known from noise measurements [24,30] to have a dramatic effect on the zero-field resistivity near the transition. The self-consistent values $m(H, 18$ K), shown as open circles in the inset of Fig. 3, match the measured critical isotherm. Neither J_{met} nor J_{ins} determines the location of the zero-field heat capacity peak at 218.2 K. Rather, the rapid buildup in both the size and number of magnetic clusters that give rise to the Griffiths behavior of the susceptibility causes a concomitant increase in the conductivity of the material. As in Griffiths' dilution picture, the existence of J_{met} serves to pull the transition temperature upward from the values expected from J_{ins} . Insofar as it is characterized by the spin-wave dispersion at low temperatures, J_{met} is essentially the same for all CMR materials. Therefore, the stronger tendency toward self-trapping that occurs as the Mn-O-Mn bond angle is reduced, lowers J_{ins} relative to J_{met} and increases the dominance of the Griffiths phase.

We have argued that the CMR effect should be treated

in the context of a Griffiths singularity driven by intrinsic randomness, the combined effect of doping, the tendency for charge segregation, and the self-trapping effect associated with polaron formation. Bray's treatment of the distribution of susceptibilities explains the unusual downturn in the measured susceptibility and the magnitude of the effective paramagnetic moment. More importantly, we have used the Griffiths idea of a distribution of exchange energies to demonstrate that the magnetic transition is driven by the accumulation of larger exchange energies on metallic bonds as the system begins to order. Magnetic fields align large clusters, turning bonds along their shared boundaries from insulating to metallic. This has the effect of shifting the effective percolation point upward in temperature, and connecting the conductive network at temperatures well above the zero-field percolation point. This is the essence of the CMR effect. A modified Oguchi model that treats pairs in the context of the double-exchange mechanism, and that uses the resistivity-derived, metallic-bond concentration, accurately captures the nature of short range correlations, although not the effect of larger clusters. Future work will address the self-consistent calculation of the concentration and magnetization without the need for empirical input from the CMR data, and will apply this analysis to other CMR transitions.

We gratefully acknowledge the contribution of Y. Tomioka and Y. Tokura in providing the sample used for this study and have benefitted from discussions with M. B. Weissman. This work was supported in part by the U.S. Department of Energy through contract DEFG02-91ER45439 in the F. Seitz Materials Research Laboratory.

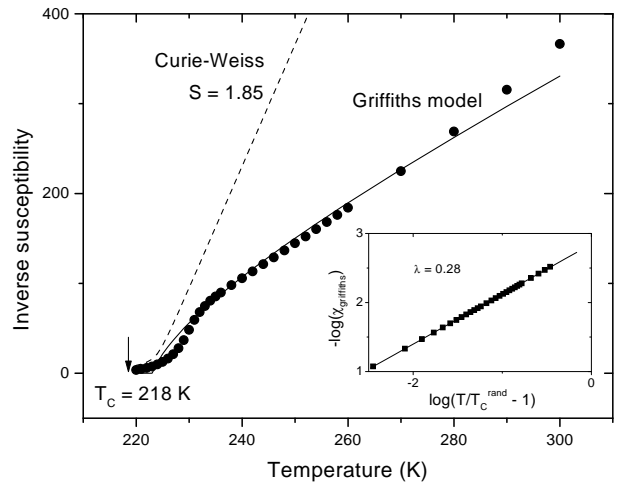


FIG. 1. Ratio of the magnetic field H to the magnetization M at 1 kOe. The dashed line is the expected Curie-Weiss behavior in a 1 kOe field for spin $S = 1.85$ and $T_C^{rand} = 223$ K while the solid line is the result of the Griffiths-phase, $H = 0$ calculation. The inset shows the Griffiths phase result vs reduced temperature on a log-log plot, demonstrating its power-law behavior.

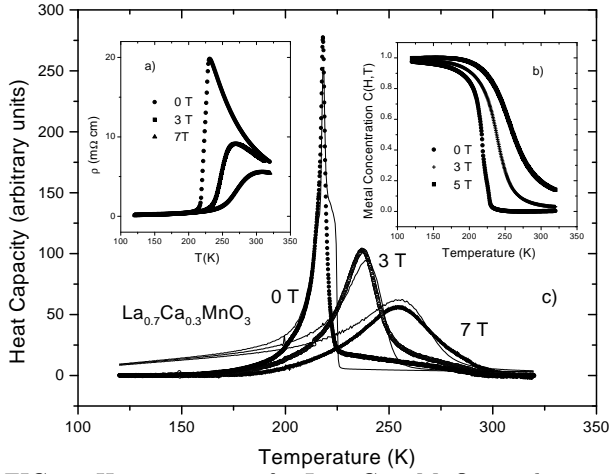


FIG. 2. Heat capacity of a $\text{La}_{0.7}\text{Ca}_{0.3}\text{MnO}_3$ single crystal at several fields. The solid lines are computed from the measured metallic-bond fraction using the Oguchi model. The resistivity and metallic fractions at the same fields are shown in insets a) and b) respectively.

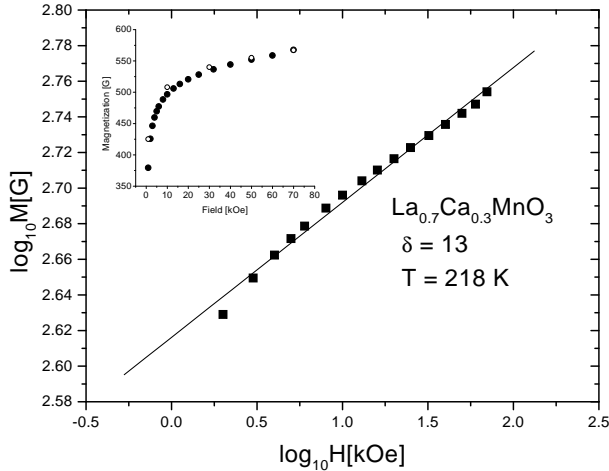


FIG. 3. Magnetization vs applied field at 218 K. The inset is a linear plot; the main panel is logarithmic, showing the small slope given by $1/\delta$. The open circles in the inset are calculated at 218 K within the Oguchi model.

-
- [1] J. Lynn *et al.*, Phys. Rev. Lett. **76**, 4046 (1996).
 - [2] P. Lin *et al.*, J. Appl. Phys. **87**, 5825 (2000).
 - [3] R. B. Griffiths, Phys. Rev. Lett. **23**, 17 (1969).
 - [4] C. Zener, Phys. Rev. **2**, 403 (1951).
 - [5] T. Okuda, Y. Tomioka, A. Asamitsu, and Y. Tokura, Phys. Rev. B **61**, 8009 (2000).
 - [6] J. J. Rhyne, (private communication, 2001).
 - [7] J. L. Garcia-Munoz, J. Fontcuberta, M. Suaaidi, and X. Obradors, J. Phys.: Cond. Matt. **8**, L787 (1996).
 - [8] J. Coey, M. Viret, and S. von Molnar, Adv. Phys. **48**, 167 (1999).
 - [9] E. Dagotto, T. Hotta, and A. Moreo, Phys. Repts. **344**, 1 (2001).
 - [10] M. Mayr *et al.*, Phys. Rev. Lett. **86**, 135 (2001).
 - [11] M. Jaime, P. Lin, S. Chun, and M. Salamon, Phys. Rev. B **60**, 1028 (1999).
 - [12] P. Dai *et al.*, Phys. Rev. Lett. **85**, 2553 (2000).
 - [13] C. P. Adams *et al.*, Phys. Rev. Lett. **85**, 3954 (2000).
 - [14] J. M. Zuo and J. Tao, Phys. Rev. B **63**, 060407 (2001).
 - [15] S. Yoon *et al.*, Phys. Rev. B **58**, 2795 (1998).
 - [16] L. P. Gor'kov and V. Z. Kresin, JEPT Letters **67**, 985 (1998).
 - [17] V. Podzorov *et al.*, Phys. Rev. B **61**, 3784 (2000).
 - [18] B. Raquet *et al.*, Phys. Rev. Lett. **84**, 4485 (2000).
 - [19] D. P. Arovas, G. Gomez-Santos, and F. Guinea, Phys. Rev. B **59**, 13569 (1999).
 - [20] A. J. Bray and M. A. Moore, J. Phys. C:Solid State Phys. **15**, L765 (1982).
 - [21] A. J. Bray, Phys. Rev. Lett. **59**, 586 (1987).
 - [22] R. Heffner *et al.*, Physica B **230**, 759 (1997).
 - [23] R. Heffner *et al.*, Phys. Rev. Lett. **85**, 3285 (2000).
 - [24] R. Merithew *et al.*, Phys. Rev. Lett. **84**, 3442 (2000).
 - [25] A. H. Castro Neto, G. Castilla, and B. A. Jones, Phys. Rev. Lett. **81**, 3531 (1998).
 - [26] J. M. De Teresa *et al.*, Nature **386**, 256 (1997).
 - [27] J. S. Smart, *Effective Field Theories of Magnetism* (W. B. Saunders, Philadelphia, 1966).
 - [28] P. Anderson and H. Hasegawa, Phys. Rev. **100**, 675 (1955).
 - [29] N. Ohata, J. Phys. Soc. Jpn **34**, 343 (1973).
 - [30] F. M. Hess *et al.*, Phys. Rev. B **63**, 180408 (2001).